SAR Pattern of Biological Objects Contacted with Coaxial Waveguide Using the FDTD Method

°Sung-Mo Koo*, Chul-Ho Won, Chang-Won Lee, and Jin-Ho Cho
Department of Radio Communication, Doowon Technical College*
Department of Electronics, Kyungpook National University

Abstract

Noninvasive multifrequency microwave radiometry using coaxial waveguide antenna has been investigated for a homogeneous and four layer human body model. The coupling between coaxial waveguide antenna and a biological object is analyzed by use of the FDTD method to obtain the absorbed power patterns in the media. The object studied in this paper is a homogeneous and four-layered lossy medium. The specific absorption rates(SAR) distribution is calculated in each region by use of the steady-state response in FDTD method.

I. Introduction

Typical tumors encountered in the clinic can range from 2 to 10 cm in diameter, and tumor sites vary from being on the skin surface to deep within the brain or pelvis. The primary objective of any hyperthermia system is to raise the temperature in the tumor volume to 43 - 55°C while the surrounding normal tissue remains below 44°C.

Noninvasive microwave radiometry has been investigated for measurement of temperature in human body. With currently available technique, invasive thermometers are used in the clinic. In this method, number and positions of thermometer probes that can be inserted in the patent's body are quite limited by trauma considerations, resulting often in inadequate thermometry. Inserting and locating the thermometer probes are laborious and time consuming tasks for doctors, besides the probe insertion gives discomfort to the patient. For these reasons, development of noninvasive technique of temperature measurement has been desired and studied for many years.

Recently, the waveguide antenna has been used in experimental investigations of multifrequency microwave radiometry to develop noninvasive techniques of constructing temperature profiles and map in biological objects[1], [2]. In these applications, the objects are lossy dielectric materials, such as a saline solution, phantom material, and a portion of human body. The portion of body coupled to the antenna is usually represented by a plane-parallel layered model consisting of, for example, the skin, fat and muscle. The problem of coupling between the rectangular waveguide antenna and the biological object of various configurations has been studied by a number of authors : Guy[3], Nikita[4], Mizoshiri[5] and Katsumi[6].

In this paper, two models of human body are considered. One is the homogeneous model which is equivalent material with human muscle and the other is the four-layered model of human body. The coupling between coaxial waveguide antenna and two model medium is analyzed by use of the FDTD method to obtain the absorbed power pattern in the medium. The SAR distribution is calculated in each region by use of the steady-state response which is obtained by observing the time history of the fields in FDTD method.

II. Description of the problem

The geometry of the problem is shown in Fig. 1, along the coordinate system, where a coaxial waveguide antenna with a finite flange is radiating into a four-layered lossy medium. The relative dielectric constant of the coaxial waveguide is $\epsilon_r = 27$ and radii of inner and outer conductor are a=2.85mm, b=28.5mm, respectively.

In our present study we treat a homogeneous lossy medium and a four-layered lossy medium. The homogeneous medium is a 0.4 % saline solution at 30°C which is considered a muscle equivalent material. The four-layered medium is assumed to consist of distilled-water(14.25mm), skin (1.9mm), fat(14.25mm) and muscle layer extending to infinity. Electrical properties of each material are listed in Table 1. Electrical properties of the saline solution and distilled-water(bolus) are obtained by Slogryan's equation[7], and those of the skin, fat and muscle are taken from Johnson and Guy[8].

The fundamental TEM mode is given at a plane normal to the waveguide axis which is 0.6λ away from coaxial end point as a source, as shown in Fig. 1, where λ is the wavelength in the coaxial waveguide. The electric field E_ρ at the reference plane is given by

$$E_\rho^i(\rho, t) = \frac{\sin \omega t}{\ln(b/a)\rho} \quad (1)$$

where ω is the angular frequency. In this paper, operating frequency is 1.2GHz. The FDTD method is used to calculate electromagnetic field in each region. Size of the cubic Yee cell is taken as $\Delta = 0.95mm \approx \lambda/30$.

III. Yee's algorithm

Yee[9] expressed Maxwell's curl equations in their finite-difference form. The Maxwell's curl equations used in the Yee/FDTD algorithm are

$$\nabla \times \underline{H} = \frac{\partial \underline{D}}{\partial t} + \underline{J}, \quad \nabla \times \underline{E} = -\frac{\partial \underline{B}}{\partial t}. \quad (2)$$

By expressing a continuous function of space and time in its discretized form, a function at its(nth) time step can be rewritten as

$$F^n(i, k) = F(i\Delta\rho, k\Delta z, n\Delta t). \quad (3)$$

After approximating the differential equations as difference equations and simplifying, following equations are obtained

$$H_\phi^{n+0.5}(i, k) = H_\phi^{n-0.5}(i, k)$$
$$+ \frac{\Delta t}{\mu_0 \Delta\rho} [E_z^n(i+0.5, k) - E_z^n(i-0.5, k)]$$
$$- \frac{\Delta t}{\mu_0 \Delta z} \left[E_\rho^n(i, k+0.5) - E_\rho^n(i, k-0.5) \right]$$

$$E_\rho^{n+1}(i, k-0.5) = \frac{1 - \frac{\sigma(i, k-0.5)}{2\epsilon(i, k-0.5)}}{1 + \frac{\sigma(i, k-0.5)}{2\epsilon(i, k-0.5)}} E_\rho^n(i, k-0.5)$$
$$- \frac{\frac{\Delta t}{\epsilon(i, k-0.5)\Delta z}}{1 + \frac{\sigma(i, k-0.5)}{2\epsilon(i, k-0.5)}} \left[H_\phi^{n+0.5}(i, k) - H_\phi^{n+0.5}(i, k-1) \right]$$

$$E_z^{n+1}(i+0.5, k) = \frac{1 - \frac{\sigma(i+0.5, k)}{2\epsilon(i+0.5, k)}}{1 + \frac{\sigma(i+0.5, k)}{2\epsilon(i+0.5, k)}} E_z^n(i+0.5, k)$$
$$- \frac{\frac{\Delta t}{\epsilon(i+0.5, k)\rho(i+0.5)\Delta\rho}}{1 + \frac{\sigma(i+0.5, k)}{2\epsilon(i+0.5, k)}} \left[\rho(i+1)H_\phi^{n+0.5}(i+1, k) \right.$$
$$\left. - \rho(i)H_\phi^{n+0.5}(i, k) \right] \quad (4)$$

where $\Delta\rho, \Delta z$ are the space increments in ρ and z directions, respectively. Δt is time increment and

meet the stability criteria as set forth by Taflove[9] and given by

$$\Delta t \leq \frac{1}{c} \sqrt{\frac{1}{\frac{1}{\Delta\rho^2} + \frac{1}{\Delta z^2}}} \quad (5)$$

IV. Absorbing boundary conditions

In order to model infinite space, boundary conditions at the computational lattice boundaries are needed. Since the computational lattice cannot be infinite for practical calculation, a finite region is used to model infinite space. When calculations stop at a fixed point in space, reflections occur at these computational boundaries. Lattice truncation conditions at the computation boundaries which simulate those of infinite space are therefore required. These absorbing boundary conditions absorb fields that are incident on the boundaries such that reflections do not occur. In our computation, the first-order absorbing boundary conditions based on Mur's ABCs[10] are used on the truncation boundaries.

V. Simulation results

In this section, results of the FDTD computation at 1.2 GHz are presented for two distinct cases:
(1) the antenna with the finite flange radiating into the homogeneous lossy medium,
(2) the antenna with the finite flange radiating into the four-layered medium.
The computation results are presented in the form of SAR distribution that in given by following equation

$$SAR(i, k) = \frac{1}{2}\sigma(i, k) \left[E_\rho^2(i, k) + E_z^2(i, k) \right], \quad (6)$$

where E_ρ and E_z are computed from the positive and negative peak values in the FDTD analysis. Fig. 2 shows SAR distribution in the homogeneous lossy medium.

Fig. 3 shows SAR distribution in the four-layered medium. The pattern indicates that the SAR distribution spread out in the lateral directions, and the spreading is much larger than in the homogeneous medium. As consequence of the lateral spreading of the radiated power, the distance of power penetration along the z-axis is smaller in the 4-layered medium (z=4.9 cm in Fig. 3) than in the homogeneous medum(z=7.9 cm in Fig. 2). The SAR distribution in the 4-layered medium is affected very strongly by the presence of bolus and fat layers.

The lateral spreading of the electric fields in the 4-layered medium may be explained as following: a

portion of the waves incident on the skin-fat and fat-muscle interfaces at oblique angles is reflected and trapped to excite waves propagating out in the lateral directons in the bolus and fat layered, and consequently in the skin layer as well. This phenomenon becomes stronger due to stronger diffraction by the antenna at lower operating frequencies. Because of this phenomenon, the depth of power penetration is slightly smaller at 1.2 GHz than at 1.8 GHz according to simulation result. This result is contrary to expectations based on a simple plane-wave theory.

VI. Conclusion

The coupling between a dielectric-filled coaxial waveguide antenna and a four-layered biological medium is analyzed by use of the FDTD method. The simulation results indicate that SAR patterns tend to spread out in the lateral directions due to the presence of the bolus and the fat layer. We are currently using the FDTD method to design a new type of coaxial waveguide antenna with proper flange dimensions to suppress the lateral spreading and to attain a deeper penetration depth of SAR distribution.

References

[1] S. Mizushina, T. Shimizu, K. Suzuki and T. Sugiura, "Retrival of temperature-depth profiles in biological objects from multifrequency microwave radiometric data," *J. of Electromagnetic Wave and Appl.*, Special issue on short-range sensing, pp. 1515-1548, 1993.

[2] F. Bardati, V. J. Brown and P. Tognolatti, " Temperature Reconstructions in a dielectric cylinder by multifrequency microwave radiometry," *J. of Electromagnetic Wave and Appl.*, Special issue on short-range sensing, pp. 1549-1571, 1993.

[3] A. W. Guy, "Electromagnetic fields and relative heating patterns due to a rectangular aperture source in direct contact with bilayered biological tissue," *IEEE Trans. Microwave Theory Tech.*, vol. MTT-19, pp. 214-223, 1971.

[4] K. S. Nikita and N. K. Uzunoglu, " Analysis of the power coupling from a waveguide hyperthermia applicator into a three-layered tissue model," *IEEE Trans. Microwave Theory Tech.*, vol. MTT-37, pp. 1794-1801, 1989.

[5] S. Mizoshiri, K. Abe, T. Sugiura and S. Mizushina, "Computation of the field distribution generated by a rectangular aperture in four-layered lossy dielectric medium by modal analysis," *IEICE Trans. Commun.*, vol. E78-B, no. 6, pp. 851-858, June 1995.

[6] K. Abe, S. Mizoshiri, T. Sugiura and S. Mizushina, "Electromagnetic near fields of a rectangular waveguide antenna in contact with biological objects obtained by the FDTD method," *IEICE Trans. Commun.*, vol. E78-B, no. 6, pp. 866-870, June 1995.

[7] S. Slogryan, "Equations for calculating the dielectric constant of saline water," *IEEE Trans. Microwave Theory Tech.*, vol. MTT-19, pp. 733-736, 1971.

[8] C. C. Johnson and A. W. Guy, "Nonionizing electromagnetic wave effects in biological materials and systems," *Proc. IEEE*, vol. 60, pp. 692-718, 1972.

[9] A. Taflove and M. E. Brodwin, "Numerical solution of steady-state electromagnetic scattering problems using the time dependent Maxwell's equations," *IEEE Trans. Microwave Theory Tech.*, vol. MTT-23, pp. 623-630, 1975.

[10] G. Mur, "Absorbing boundary conditions for the finite difference approximation of the time-domain electromagnetic field equations," *IEEE Trans. Electromag. Compat.*, vol. EMC-23, pp. 377-382, 1981.
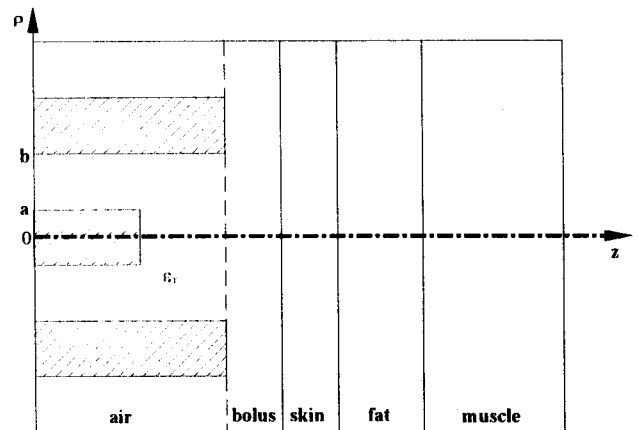
Fig.1 Geometry of a coaxial waveguide antenna with a finite flange in contact with a 4-layered object

Table 1. Electrical properties of biological materials
at 1.2GHz

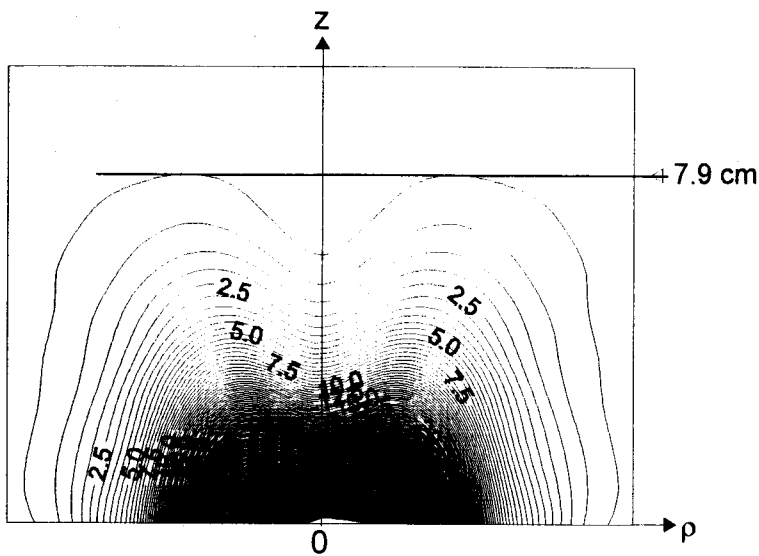|	dielectric constant	conductivity (S/m)
0.4 % saline solution(30°C)	75.1	1.0
skin	49.7	1.7
fat	5.6	0.16
muscle	49.7	1.7
bolus (distilled-water)	76.4	0.26

Fig.2 SAR distribution in a homogeneous lossy
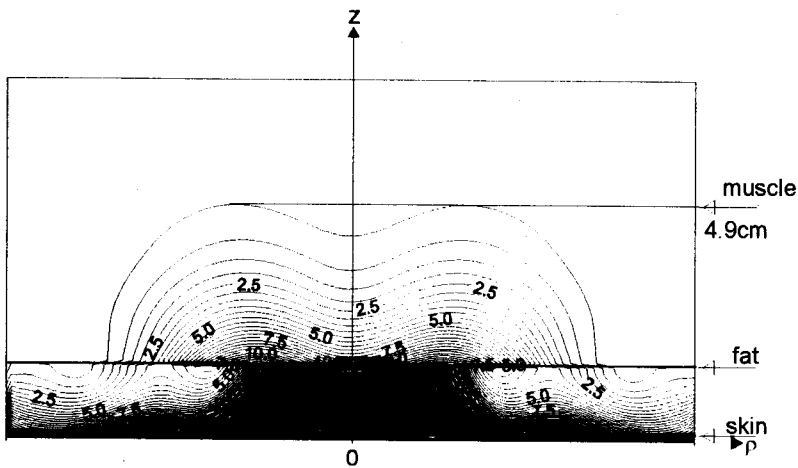medium for the antenna with finite flange

Fig.3 SAR distribution in the 4-layered medium for
a antenna with the finite flange